CPT-BASED LIQUEFACTION TRIGGERING PROCEDURE

by

Ross W. Boulanger, Professor, F. ASCE
(Corresponding author: rwboulanger@ucdavis.edu; (530) 752-2947)
Department of Civil and Environmental Engineering
University of California, Davis CA 95616

I. M. Idriss, Professor Emeritus, Distinguished M. ASCE
Department of Civil and Environmental Engineering
University of California, Davis CA 95616

Submitted
September 2014
Revised March 22, 2015
Finalized June 2, 2015

Abstract

A probabilistic cone penetration test (CPT) based liquefaction triggering procedure for cohesionless soils is derived using a maximum likelihood method with an updated case history database. The liquefaction analysis framework includes revised relationships for the magnitude scaling factor (MSF) and for estimating fines contents from CPT data when laboratory test data are not available. The updated case history database and methodology for developing the liquefaction correlation are described. Measurement and estimation uncertainties, the potential effects of false positives and false negatives in the case history database, and the effects of the choice-based sampling bias in the case history database are accounted for. Sensitivity analyses showed that the position of the most likely triggering curve and the magnitude of the total error term are reasonably well constrained by the data. The sensitivity study provides reasonable bounds on the effects of different interpretations, from which probabilistic and deterministic relationships for practice are recommended.

Key Words: Liquefaction, earthquakes, cyclic loads, standard penetration test, probability.

Introduction

Cone penetration test (CPT) and Standard Penetration Test (SPT) based probabilistic correlations for evaluating liquefaction triggering in cohesionless soils have advanced through the contributions of numerous researchers (e.g., Christian and Swiger 1975, Liao et al. 1988, Liao and Lum 1998, Youd and Nobel 1997, Toprak et al. 1999, Juang et al. 2002, Cetin et al. 2004, Moss et al. 2006, Boulanger and Idriss 2012). Some probabilistic relationships represent the total uncertainty in the evaluation of the case history database; i.e., they include the uncertainty in the triggering relationship (model uncertainty) and the uncertainty in the representative $(N_1)_{60cs}$ or q_{c1Ncs} and $CSR_{M=7.5,\sigma'=1}$ values determined for the case histories (measurement or parameter uncertainty). The approach developed by Cetin et al. (2002) allowed for a separate accounting of the model and measurement uncertainties. For applications, the total uncertainty will include contributions from the liquefaction triggering model and input parameters. The parameter uncertainties in an application are not necessarily the same as the measurement uncertainties in the case history database, and thus it is important to have separately quantified the model uncertainty so that it can be rationally combined with the parameter uncertainties in a probabilistic liquefaction evaluation.

The quantity and quality of CPT and SPT case histories has increased with recent earthquake events, including data obtained in the 2010-2011 Canterbury earthquake sequence in New Zealand (e.g., van Ballegooy et al. 2014, Green et al. 2014) and the 2011 M_w=9.0 Tohoku earthquake in Japan (e.g., Tokimatsu et al. 2012, Cox et al. 2013). For example, Green et al. (2014) compiled 50 case histories representing cases of liquefaction and no liquefaction during the 2010-2011 Canterbury earthquake sequence with subsurface profiles for which the critical layer could be identified with relatively high confidence. The inclusion of these and other data provide an opportunity for re-evaluating liquefaction triggering procedures and updating them as warranted.

In this paper, a probabilistic CPT-based liquefaction triggering procedure for cohesionless soils is derived using a maximum likelihood method and an updated case history database. The liquefaction analysis framework is described, including revised relationships for magnitude scaling factor (MSF) and for estimating fines contents from CPT data when laboratory test data are not available. The updated case history database and methodology for developing the probabilistic relationships for liquefaction triggering are described. The sensitivity of the maximum likelihood solution to various assumptions regarding measurement uncertainties and the potential influence of false positive or false negative case histories in the database are evaluated.

A probabilistic correlation is then proposed and issues regarding its use in practice are discussed. Details for each of these steps are presented in Boulanger and Idriss (2014).

Liquefaction Analysis Framework

The liquefaction analysis framework follows that by Idriss and Boulanger (2008) and incorporates changes to the MSF and procedures for estimating FC from CPT data when laboratory test data are not available. The functional terms provide the means for rationally interpreting case histories and extending the resulting correlation to conditions outside those covered by the case history database. An outcome of the triggering correlation is a FC adjustment relationship, which is presented in this section to facilitate presentation of the case history database in a common format.

The earthquake-induced cyclic stress ratio (CSR), at a given depth, z, within the soil profile, is expressed as a representative value equal to 65% of the maximum cyclic shear stress ratio, i.e.:

$$CSR_{M,\sigma'_v} = 0.65\frac{\tau_{max}}{\sigma'_v} \tag{1}$$

where τ_{max} = maximum earthquake induced shear stress, σ'_v = vertical effective stress, and the subscripts on the CSR indicate that it is computed for a specific earthquake magnitude (moment magnitude, M) and in-situ σ'_v. The value of τ_{max} can be estimated from dynamic response analyses, but such analyses must include a sufficient number of input acceleration time series and adequate site characterization details to be reasonably adequate. Alternatively, the maximum shear stress can be estimated using the Seed-Idriss Simplified Procedure to arrive at,

$$CSR_{M,\sigma'_v} = 0.65\frac{\sigma_v}{\sigma'_v}\frac{a_{max}}{g}r_d \tag{2}$$

where σ_v = vertical total stress at depth z, a_{max}/g = maximum horizontal acceleration (as a fraction of gravity) at the ground surface, and r_d = shear stress reduction factor that accounts for dynamic response of the soil profile. The expression for r_d by Idriss (1999), as derived from site response analyses, was used in the present study as,

$$r_d = \exp\left[\alpha(z) + \beta(z) \cdot M\right] \tag{3a}$$

$$\alpha(z) = -1.012 - 1.126 \sin\left(\frac{z}{11.73} + 5.133\right) \tag{3b}$$

$$\beta(z) = 0.106 + 0.118 \sin\left(\frac{z}{11.28} + 5.142\right) \tag{3c}$$

where z = depth below the ground surface in meters and the arguments inside the sin terms are in radians. Additional details on development of this relationship are in Idriss and Boulanger (2010).

CPT penetration resistances are corrected for overburden stress effects as,

$$q_{c1N} = C_N q_{cN} = C_N \frac{q_c}{P_a} \tag{4}$$

where C_N = overburden correction factor, P_a = atmospheric pressure (101.3 kPa, 1 atm), $q_{cN} = q_c/P_a$, and q_{c1N} is the penetration resistance that would be obtained in the same sand at an overburden stress of 1 atm if all other attributes remain constant (e.g., same relative density, fabric, age, degree of cementation, loading history). Note that q_c should be corrected for pore pressures measured behind the tip whenever such data are available. The C_N relationship by Boulanger (2003) based on calibration chamber test data and numerical modeling of cone penetration was used,

$$C_N = \left(\frac{P_a}{\sigma'_v}\right)^m \leq 1.7 \tag{5a}$$

$$m = 1.338 - 0.249\left(q_{c1Ncs}\right)^{0.264} \tag{5b}$$

where q_{c1Ncs} = equivalent clean sand penetration resistance (as discussed below). The exponent m can be constrained to its recommend limits of $0.264 \leq m \leq 0.782$ by limiting q_{c1Ncs} values to between 21 and 254 for use in these expressions.

The soil's cyclic resistance ratio (CRR) is dependent on the duration of shaking (expressed through the MSF) and σ'_v (expressed through a K_σ factor). The correlation for CRR is therefore developed by adjusting the case history CSR values to a reference M = 7.5 and σ'_v = 1 atm as,

$$CSR_{M=7.5,\sigma'_v=1} = \frac{CSR_{M,\sigma'_v}}{MSF \cdot K_\sigma} \tag{6}$$

The soil's CRR is further affected by the presence of sustained static shear stresses, such as may exist beneath foundations or within slopes. The effect of sustained static shear stresses, expressed through a K_α factor, is generally small for nearly level ground conditions and is not included herein because the case history database is dominated by level or nearly level ground conditions.

The K_σ relationship by Boulanger (2003), which was based on a compilation of experimental data interpreted in a critical-state framework, was used as

$$K_\sigma = 1 - C_\sigma \ln\left(\frac{\sigma'_v}{P_a}\right) \leq 1.1 \tag{7a}$$

$$C_\sigma = \frac{1}{37.3 - 8.27\left(q_{c1Ncs}\right)^{0.264}} \leq 0.3 \tag{7b}$$

The coefficient C_σ can be limited to its maximum value of 0.3 by restricting q_{c1Ncs} to ≤ 211 in these expressions. The above relationships have been shown to be in reasonable agreement with an updated database of laboratory experimental data by Montgomery et al. (2014).

The MSF by Boulanger and Idriss (2014, 2015), derived from a compilation of laboratory test data and analyses of ground motion recordings, includes dependency on soil characteristics as

$$MSF = 1 + \left(MSF_{max} - 1\right)\left(8.64\, exp\left(\frac{-M}{4}\right) - 1.325\right) \tag{8}$$

where MSF_{max} was related to q_{c1Ncs} values as,

$$MSF_{max} = 1.09 + \left(\frac{q_{C1Ncs}}{180}\right)^3 \leq 2.2 \tag{9}$$

The resulting MSF relationship for different values of q_{c1Ncs} is shown in Fig. 1. This relationship produces MSF_{max} = 1.8 at $q_{c1Ncs} \approx 160$, which matches the MSF relationship for sand by Idriss (1999), and $MSF_{max} \approx 1.10$ for $q_{c1Ncs} < 60$, which is consistent with the expected results for very loose sands or soft low-plasticity silts.

The correlation of CRR to q_{c1N} in cohesionless soils is also affected by the soil's FC. For mathematical convenience, this correlation can also be expressed in terms of an equivalent clean-sand q_{c1Ncs} values which are obtained using the following expressions:

$$q_{c1Ncs} = q_{c1N} + \Delta q_{c1N} \tag{10}$$

$$\Delta q_{c1N} = \left(11.9 + \frac{q_{c1N}}{14.6}\right)\exp\left(1.63 - \frac{9.7}{FC+2} - \left(\frac{15.7}{FC+2}\right)^2\right) \tag{11}$$

The equivalent clean-sand adjustment $\Delta q_{c1N} = f(FC)$ is derived so that CRR can be expressed as a function of q_{c1Ncs} alone and thus Δq_{c1N} accounts for the effect that FC has on both CRR and q_{c1N}. The Δq_{c1N} relationship (Fig. 2) is primarily based on its empirical fit to the liquefaction case history data, but the sparseness of the case history data for combinations of high q_{c1N} and high FC values (as described later) provide limited constraint on the shape (form) of the relationship. For this reason, the selection of its form was also guided by checking consistency of the resulting CPT-based probabilistic triggering correlation with the SPT-based probabilistic correlation by Boulanger and Idriss (2012) in terms of implied q_c/N_{60} ratios and relative state parameter indices for common values of $CRR_{M=7.5,\sigma'=1atm}$ and probability of liquefaction (P_L). The adopted forms for the $\Delta q_{c1N} = f(FC)$ and $CRR_{M=7.5,\sigma'=1atm} = f(q_{c1Ncs})$ equations were chosen to produce q_c/N_{60} ratios which are in reasonable agreement with Suzuki et al.'s (1998) empirical data for q_c/N_{60} ratios in sands and silty sands, including the trends for q_c/N_{60} to decrease with increasing relative density and increasing FC (details in Boulanger and Idriss 2014). The adjustments begin to plateau for FC values exceeding about 35% because the soil matrix is believed to become fines-dominated for any FC value greater than about this value. The adjustments are considered appropriate for nonplastic to low-plasticity silty fines. The adjustments are presented here because they are used in the following sections for summarizing the case history data and examining their distributions across a range of conditions.

Soil Classification Estimation using CPT data

The FC and soil classification are often correlated to a soil behavior type index (I_c) which is a function of the q_c and sleeve friction ratio (f_s). The I_c term by Robertson and Wride (1998) is,

$$I_c = \left[\left(3.47 - \log(Q)\right)^2 + \left(1.22 + \log(F)\right)^2\right]^{0.5} \quad (12)$$

where Q and F are normalized tip and sleeve friction ratios computed as,

$$Q = \left(\frac{q_c - \sigma_{vc}}{P_a}\right)\left(\frac{P_a}{\sigma'_{vc}}\right)^n \quad (13)$$

$$F = \left(\frac{f_s}{q_c - \sigma_{vc}}\right) \cdot 100\% \quad (14)$$

The exponent n varies from 0.5 in sands to 1.0 in clays (Robertson and Wride 1998).

General correlations between FC and I_c or other CPT-based indices exhibit large scatter, such that site-specific calibration or checking of such correlations is strongly encouraged. The relationship for estimating FC herein is,

$$\begin{aligned} &FC = 80\left(I_C + C_{FC}\right) - 137 \\ &0\% \le FC \le 100\% \end{aligned} \quad (15)$$

where C_{FC} is a fitting parameter (default value is 0.0). This expression with C_{FC} = 0.0, -0.29, and 0.29 (i.e., ± an amount equal to the standard deviation in the general correlation) is shown in Fig. 3. Site specific calibration of C_{FC} should be for individual geologic strata (common source material, deposition, etc.), such that different C_{FC} values may be obtained for different strata at any one site. For example, setting C_{FC} = -0.07 is approximately equal to the relationship developed by Robinson et al. (2013) for liquefiable soils along the Avon River in Christchurch, New Zealand.

Ground densification work has been observed to change the FC-I_c correlation at specific sites through its effects on q_c and f_s, with the result that C_{FC} may be different before and after ground densification work (e.g., Nguyen et al. 2014). Similarly, the I_c value used to distinguish clays from sands has often been observed to decrease as a result of densification. The consistency of the inferred soil profile characteristics from before to after ground densification can be used to develop site-specific adjustments in both C_{FC} and the I_c cut-off value.

A CPT-based liquefaction triggering evaluation should consider the uncertainty in FC and soil classification estimates when site-specific sampling and lab testing data are not available. For example, liquefaction analyses could be repeated using a range of C_{FC} values to evaluate the sensitivity to FC estimates; e.g., using C_{FC} = ±0.15 or ±0.29 would allow for about ±½ or 1 standard deviation in this relationship. Similarly, the I_c cut-off value used to screen out clay-like soils is commonly taken as 2.6 but other values may be justified based on site specific sampling and testing (Robertson and Wride 1998). Liquefaction analyses could be repeated using I_c cut-off values of 2.4 and 2.6 to evaluate sensitivity to this parameter. Results of such analyses can be used to evaluate potential benefits of site-specific sampling and testing, while recognizing that some amount of sampling and testing should always be required for high risk/high consequence projects.

CPT-based Case History Database

A database of CPT liquefaction case histories is updated, including adding data from recent earthquake events (e.g., PEER 2000a,b, Sancio 2003, Green et al. 2014, Cox et al. 2013). The individual case histories and key references are summarized in Table S1 in the electronic supplement. We examined the original sources for all cases, as well as interpretations by others (e.g., Moss et al. 2003), to obtain independent interpretations consistent with our current understanding and judgments. For cases where our interpretation was within a few percent of the original investigators, we retained the interpretation of the original investigator.

The available information for most case histories with I_c near 2.6±0.2 (i.e., 2.4 to 2.8) in critical strata is insufficient to confidently evaluate whether the soils would be best analyzed with a liquefaction triggering framework (i.e., that for sands) or a cyclic softening framework (i.e., that for clays or silts with high PI). The cases listed in Table S1 are nonetheless limited to cases with $I_c < 2.6$, recognizing this assumes a priori the adequacy of this criterion for identifying the most appropriate analysis framework. Of the 253 cases listed in Table S1, 180 cases had surface evidence of liquefaction, 71 cases had no surface evidence of liquefaction, and 2 cases were described as being at the margin between liquefaction and no liquefaction.

Moment magnitudes (M or M_w) are used for all earthquakes (Table S1). The M were obtained from the Next Generation Attenuation NGA-2 project flatfile (Ancheta et al. 2014) and USGS Centennial Earthquake Catalog (Engdahl and Villasenor 2002, and online catalog 2010).

Estimates of peak horizontal ground accelerations (PGA or a_{max}) are listed for each site in Table S1. PGA estimates by the original site investigators or from the Moss et al. (2003) database were used in all cases except as noted below. USGS ShakeMaps (Worden et al. 2010) were used to check PGA estimates for a number of sites with no nearby recordings, as described in Boulanger and Idriss (2014). In practice, the use of a geometric mean a_{max} in assessing liquefaction hazards is considered to be a reasonable engineering approach for many geotechnical structures (e.g., levees, embankment dams) or soil-structure systems (e.g., bridge abutments, pipelines) which often have direction-dependent response characteristics.

A number of CPT-based case histories are discussed in Boulanger and Idriss (2014) to illustrate issues important to the interpretation of case histories, including the geologic understanding of the site and methodology used for selecting representative q_{c1Ncs} values from critical strata. In general, the appropriateness of any averaging of q_{cN} values for a specific stratum in case history interpretations or forward analyses depends on the spatial characteristics of the stratum (e.g., thickness, lateral extent, continuity, variability), the mode of deformation (e.g., reconsolidation settlement, lateral spreading, slope instability), and the spatial dimensions of the potential deformation mechanisms relative to the strata of concern. A familiarity with how representative q_{c1Ncs} values are selected for the database is important for guiding the forward application of these correlations in a manner consistent with their development.

Site performance during an earthquake is classified as a "liquefaction", "no liquefaction", or "marginal" case. Cases described as "liquefaction" were generally accompanied with reports of sand boils and/or visible ground surface settlements, cracks, or lateral movements. Cases described as "no liquefaction" were generally accompanied with reports of no visible surface manifestations. Two cases were classified as "marginal" because the available information suggests that conditions at the site are likely at, or near, the boundary of conditions that separate the physical occurrence of liquefaction from non-liquefaction.

Distribution of data

The distributions of the case history data are illustrated in Figs. 4 and 5. Plots of q_{cN} and F versus representative depth of the critical zone (Fig. 4) show the database is limited to average critical depths less than 12 m with few points for average depths greater than about 9 m. Plots of M versus a_{max} (Fig. 5a) show the current database includes few cases for M less than 6 or greater than 7.6. Plots of q_{cN} versus FC (Fig. 5b) show there are relatively few cases with high FC and essentially no cases with both high FC and high q_{cN} values. Explicit statements regarding the plasticity of the fines fraction [i.e., a plasticity index (PI) or statement that the fines are nonplastic] are not provided for most case histories, but the available information and descriptions suggest they correspond primarily to soils with nonplastic or low plasticity silty fines. Additional figures illustrating the distribution of the case history parameters are provided in the electronic Supplement.

Liquefaction analyses should evaluate how the conditions of a specific project compare to the conditions covered by the case history database. If project conditions fall outside those constrained by case history data, then the results of liquefaction triggering analyses using different correlations can be strongly dependent on the functional relationships used within those correlations. In such cases, a clear understanding of the bases behind the functional relationships can be important for guiding judgments regarding the applicability of the results so obtained.

Probabilistic Relationship for CPT-based Triggering Procedure

The probabilistic triggering correlation was developed using a maximum likelihood method that utilizes the forms of the limit state and likelihood functions used by Cetin et al. (2002, 2004). Emphasis is placed on developing a reasonable first-order estimate of the total and model uncertainties given that the available case history data are insufficient for quantifying the components of uncertainty on a site-by-site basis. Measurement and estimation uncertainties, the potential effects of false positives and false negatives in the case history database, and the effects of the choice-based sampling bias in the case history database are accounted for. The sensitivity of the maximum likelihood solution to subsets of the database and to a range of estimated measurement uncertainties is evaluated, from which relationships for practice are recommended.

Limit state function

The limit state function (g) was taken as the difference between the natural logs of $CRR_{M=7.5,\sigma'=1atm}$

and $CSR_{M=7.5,\sigma'=1atm}$, such that liquefaction is assumed to have occurred if $g \leq 0$ and to have not occurred if $g > 0$. The $CRR_{M=7.5,\sigma'=1atm}$ value was estimated using the following relationship,

$$CRR_{M=7.5,\sigma'_v=1atm} = \exp\left(\frac{q_{c1Ncs}}{113} + \left(\frac{q_{c1Ncs}}{1000}\right)^2 - \left(\frac{q_{c1Ncs}}{140}\right)^3 + \left(\frac{q_{c1Ncs}}{137}\right)^4 - C_o\right) \quad (16)$$

where C_o is an unknown fitting parameter that serves to scale the relationship while maintaining its shape. This relationship is not tightly constrained by the case history data for low or high values of q_{c1Ncs}, and thus its shape was also guided by checking its consistency with the SPT-based correlation by Boulanger and Idriss (2012) in terms of implied q_c/N_{60} ratios and relative state parameter indices for common values of $CRR_{M=7.5,\sigma'=1atm}$ and P_L. The form of Equation 16 was shown to produce q_c/N_{60} ratios which are in reasonable agreement with the Suzuki et al.'s (1998) empirical data for sands including the trend for q_c/N_{60} to decrease with increasing relative density (Boulanger and Idriss 2014). The limit state function can then be written as,

$$\hat{g}\left(q_{c1Ncs}, C_o, CSR_{M=7.5,\sigma'_v=1atm}\right) = \ln\left(CRR_{M=7.5,\sigma'_v=1atm}\right) - \ln\left(CSR_{M=7.5,\sigma'_v=1atm}\right) \quad (17)$$

where the hat on g indicates that it is imperfect in its prediction of liquefaction.

The uncertainties in the limit state function are represented by three contributors. Measurement or estimation uncertainties in the case history data points are assumed to be adequately represented by including uncertainties in the q_{c1Ncs} and $CSR_{M=7.5,\sigma'=1atm}$ values. The uncertainty in q_{c1Ncs} is assumed to be normally distributed with a constant coefficient of variation (COV) (e.g., Baecher and Christian 2003). The uncertainty in $CSR_{M=7.5,\sigma'=1atm}$ is assumed to be log-normally distributed, which is consistent with log-normal distributions for the uncertainty in predictions of peak ground accelerations (e.g., Abrahamson et al. 2008). Uncertainty in the $CRR_{M=7.5,\sigma'=1atm}$ expression is represented by inclusion of a random model error term, which is assumed to also be log normally distributed with mean of zero.

The uncertainty in the representative q_{c1Ncs} value assigned to any case history includes contributions from three major sources. One source is the degree to which the available CPT data are representative of the critical strata, which depends on the degree to which the geologic conditions are understood, the heterogeneity of the deposits, the number of soundings, and the placement of the soundings relative to the strata of concern. A second source of uncertainty is the CPT-based estimation of soil types (e.g., FC and fines plasticity), which depends on the availability and quality of site-specific sampling and index testing data. A third source of uncertainty is variability in the CPT equipment and procedures used at different case history sites. The coefficient of variation (COV) of q_{c1N} measurements in sand have been reported to range from 0.20 to 0.60 with a mean of about 0.38 (Kulhawy and Trautmann 1996, Phoon and Kulhawy 1999). The large majority of the liquefaction case histories lack sufficient information to justify site-specific estimates of the uncertainty in the representative q_{c1Ncs} values. For this reason, the COV was taken as being the same for all case histories where FC and fines plasticity are based on site-specific sampling and index testing and to be 50% greater when site-specific sampling and index testing data are not available. The 50% increase in the uncertainty for cases without site-specific sampling and index test data is a subjective adjustment based on considering how potential differences in FC adjustments (Δq_{c1N}) would affect estimates of q_{c1Ncs}. Parametric analyses were then used to assess the sensitivity of the solution to the assumed values for the COV.

The uncertainty in the $CSR_{M=7.5,\sigma'=1atm}$ values estimated for any case history similarly depends on numerous factors, including the proximity of strong ground motion recordings, potential variability in site responses, availability and quality of indirect measures of shaking levels (e.g., eye witness reports, damage to structures, disruption of nonstructural contents), variability in the ground motion characteristics (e.g., duration of shaking), and the overburden stress. Ground

Submitted September 2014
Revised March 22, 2015

motion prediction equations (GMPEs) have standard deviations of about 0.45-0.55 in the natural log of a_{max} (Abrahamson et al. 2008), which implies similar uncertainty in the CSR if it was estimated on the basis of a GMPE. The case history estimates of a_{max} by various researchers are usually based on several sources of information as discussed above, and likely have smaller variances than estimates obtained from GMPEs alone. The available data is, however, inadequate for quantifying the uncertainty in $CSR_{M=7.5,\sigma'=1atm}$ on a case-history specific basis. For this reason, the standard deviation in $\ln(CSR_{M=7.5,\sigma'=1atm})$ was set to: (1) the small value of 0.05 for the few sites that had strong ground motion recordings directly at the site, to allow for uncertainty in the MSF, K_σ, and r_d terms even when a_{max} is known, and (2) a relatively greater value for all other sites. The sensitivity of the solution to a range of values in this latter parameter is presented in a later section.

Notation

It is convenient to simplify the notation as follows,

$$Q = q_{c1Ncs} \tag{18}$$

$$S = CSR_{M=7.5,\sigma'_v=1atm} \tag{19}$$

$$R = CRR_{M=7.5,\sigma'_v=1atm} \tag{20}$$

The limit state function can be written using a total error term ε_T, to account for both the inability of $\hat{g}$ to predict liquefaction perfectly and the uncertainty in the parameters used to compute $\hat{g}$.

$$g\left(Q, S, C_o, \varepsilon_{\ln(R)}\right) = \hat{g}\left(\hat{Q}, \hat{S}, C_o\right) + \varepsilon_T \tag{21}$$

The ε_T is normally distributed with a mean value of zero and includes the effects of uncertainty in the parameters, which are expressed as,

$$Q = \hat{Q} + \varepsilon_Q \tag{22}$$

$$\sigma_Q = COV_Q \cdot \hat{Q} \tag{23}$$

$$\ln\left(S\right)=\ln\left(\hat{S}\right)+\varepsilon_{\ln(S)} \quad (24)$$

$$\ln\left(R\right)=\ln\left(\hat{R}\right)+\varepsilon_{\ln(R)} \quad (25)$$

The limit state function and the total error can then be expressed as,

$$g\left(Q,S,C_o,\varepsilon_{\ln(R)}\right)=\hat{g}\left(\hat{Q},\hat{S},C_o\right)+\left(\frac{1}{113}+\frac{2\hat{Q}}{1000^2}-\frac{3\hat{Q}^2}{140^3}+\frac{4\hat{Q}^3}{137^4}\right)\varepsilon_Q+\varepsilon_{\ln(R)}-\varepsilon_{\ln(S)} \quad (26)$$

$$\varepsilon_T=\left(\frac{1}{113}+\frac{2\hat{Q}}{1000^2}-\frac{3\hat{Q}^2}{140^3}+\frac{4\hat{Q}^3}{137^4}\right)\varepsilon_Q+\varepsilon_{\ln(R)}-\varepsilon_{\ln(S)} \quad (27)$$

The standard deviation in ε_T can be expressed as,

$$\left(\sigma_T\right)^2=\left(\frac{1}{113}+\frac{2\hat{Q}}{1000^2}-\frac{3\hat{Q}^2}{140^3}+\frac{4\hat{Q}^3}{137^4}\right)^2\left(\sigma_Q\right)^2+\left(\sigma_{\ln(R)}\right)^2+\left(\sigma_{\ln(S)}\right)^2 \quad (28)$$

Likelihood function

The likelihood function is the product of the probabilities of the individual case history observations, assuming that the case history observations are statistically independent. For a liquefaction case ($g \leq 0$), the probability of having observed liquefaction can be expressed as,

$$P\left[g\left(Q,S,C_o,\varepsilon_{\ln(R)}\right)\leq 0\right]=\Phi\left[-\frac{\hat{g}\left(\hat{Q},\hat{S},C_o\right)}{\sigma_T}\right] \quad (29)$$

where Φ is the standard normal cumulative probability function. For example, the probability of having observed liquefaction is greater than 0.84 if the data point plots more than one σ_T above the triggering curve. Case history data points for sites without ground motion recordings (almost all of them) are plotted at the $CSR_{M=7.5,\sigma'=1atm}$ value expected in the absence of liquefaction, and this $CSR_{M=7.5,\sigma'=1atm}$ value may be greater than the value which was developed if liquefaction was triggered early in strong shaking. For this reason, the data points that fall well above the triggering curve have probabilities close to unity, and thus have little influence on the overall likelihood function. The same is true for the no-liquefaction cases that fall well below the triggering curve.

The case history database is believed to contain an uneven sampling of liquefaction and no-liquefaction case histories because researchers more often have chosen to investigate liquefaction sites. Manski and Leman (1977) suggest that the bias from an uneven choice-based sampling process can be corrected for by weighting the observations to better represent the actual population. Cetin et al. (2002) noted that this amounted to writing the likelihood function as,

$$L\left(C_o, \varepsilon_{\ln(R)}\right) = \prod_{Liquefied\ sites} \Phi\left[-\frac{\hat{g}\left(\hat{Q}, \hat{S}, C_o\right)}{\sigma_T}\right]^{w_{liquefied}} \prod_{Noniquefied\ sites} \Phi\left[\frac{\hat{g}\left(\hat{Q}, \hat{S}, C_o\right)}{\sigma_T}\right]^{w_{nonliquefied}} \quad (30)$$

where the exponents $w_{liquefied}$ and $w_{nonliquefied}$ used to weight the observations are computed as,

$$w_{liquefied} = \frac{Q_{liq,true}}{Q_{liq,sample}} \quad (31)$$

$$w_{nonliquefied} = \frac{1 - Q_{liq,true}}{1 - Q_{liq,sample}} \quad (32)$$

where $Q_{liq,true}$ is the true proportion of the occurrences of liquefaction in the population, and $Q_{liq,sample}$ is the proportion of occurrences of liquefaction in the sample set. Cetin et al. (2002) adopted weighting values of $w_{liquefied}$ = 0.8 and $w_{nonliquefied}$ = 1.2, producing the ratio $w_{nonliquefied}/w_{liquefied}$ = 1.5. Moss et al. (2006) used these same weighting parameters in their application of this procedure to their CPT-based liquefaction triggering database. These same values are used herein, except as otherwise noted.

The case history database likely contains a number of false negatives and false positives because the true site performance is either masked or mischaracterized. A scenario of concern for false negatives is when liquefaction at depth does not produce any visible surface manifestation, such as may occur when a thick crust of non-liquefiable soil overlies a relatively thin zone of liquefaction and there is no significant slope or heavy structure to induce deformations. False positives are not expected to be as common, but it is possible that ground surface cracking or settlement could result from seismic compression of unsaturated loose soils or yielding of soft clays (e.g., bearing failures around buildings), and that such movements could be interpreted as having been caused by liquefaction of a different strata at the site. The potential exists for false positives or false negatives to produce points that fall far from the triggering correlation, which would be incorrectly treated as highly unlikely cases in the maximum likelihood solution. The influence of such outliers was minimized by limiting the probability of any one observation to be no smaller than a specified minimum value, P_{min}. Sensitivity analyses considered values of P_{min} = 0, 0.05, 0.075, and 0.10, as well as an alternative approach where outlier points were omitted.

Maximum Likelihood Solutions

Maximum likelihood solutions for the triggering correlation were obtained for several subsets of the case history database, including: (1) clean sand (FC ≤ 5%) case histories, (2) case histories where the FC is based on laboratory test data alone, (3) all case histories whether the FC was based on laboratory test data or correlation with I_c, and (4) all case histories with σ'_v greater than 40 kPa. For each subset, solutions were obtained using ranges for the estimation parameters: $\sigma_{ln(S)}$, COV_Q, $w_{nonliquefied}/w_{liquefied}$, and P_{min}. In addition, the total uncertainty σ_T at high q_{c1Ncs} values was limited to ≤0.6 except as otherwise noted. Results of these analyses are in Boulanger and Idriss (2014), from which representative results are used to illustrate the primary observations.

Solutions based on the clean sand (FC ≤ 5%) case histories are plotted with the clean sand case history data in Fig. 6 for P_{min} = 0.0 (i.e., no allowance for false negatives or false positives) and Fig. 7 for P_{min} = 0.05. Curves for probabilities of liquefaction [P_L] equal to 15%, 50%, and 85% in

Submitted September 2014
Revised March 22, 2015

terms of the total uncertainty, which means with inclusion of the estimation errors in $CSR_{M=7.5,\sigma'=1atm}$ and q_{c1Ncs}, are shown in both figures for three scenarios: (a) $\sigma_{ln(S)}$ = 0.2, COV_Q = 0.2, (b) $\sigma_{ln(S)}$ = 0.15, COV_Q = 0.15, and (c) $\sigma_{ln(S)}$ = 0.1, COV_Q = 0.1. The P_L = 50% curves for the three scenarios are on top of each other in each figure, showing that the expected position of the triggering correlation is insensitive to the estimated values of $\sigma_{ln(S)}$ and COV_Q. The P_L = 15% and 85% curves for the three scenarios in either figure show only small differences, indicating that the total uncertainty in the triggering correlation is also relatively insensitive to the estimated values of $\sigma_{ln(S)}$ and COV_Q. Comparing the solutions in Figs. 6 and 7, the use of P_{min} = 0.05 produced a slightly lower median curve (about 5% lower) and smaller total uncertainty terms (e.g., the P_L = 15% and 85% curves are located closer together). Setting P_{min} = 0.05 rather than to 0.0 reduced the influence of the two or three no-liquefaction data points located well above the expected triggering correlation (Figs. 6 or 7), which is why the most likely triggering curve shifted down slightly and the total uncertainty terms were reduced.

Solutions based on all the case histories are plotted together with the case history data: (1) in Fig. 8 in terms of the total uncertainty, and (2) in Fig. 9 in terms of model uncertainty alone, which means excluding the estimation errors in $CSR_{M=7.5,\sigma'=1atm}$ and q_{c1Ncs}. Curves for P_L = 15%, 50%, and 85% are shown in both figures for P_{min} = 0.075 and the same $\sigma_{ln(S)}$ and COV_Q scenarios as used above. The P_L = 15% and 85% curves based on total uncertainty (Fig. 8) are again insensitive to the estimated values of $\sigma_{ln(S)}$ and COV_Q. The total uncertainties for these scenarios, as plotted in Fig. 10, were similar because decreasing the assumed values for $\sigma_{ln(S)}$ and COV_Q was offset by increases in the most likely values for $\sigma_{ln(R)}$; e.g., decreasing $\sigma_{ln(S)}$ and COV_Q from 0.2 to 0.1 caused $\sigma_{ln(R)}$ to increase from 0.05 to 0.24 as listed in the legend of Fig. 10. The P_L = 15% and 85% curves based on model uncertainty alone (Fig. 9) move progressively closer together with increasing

Submitted September 2014
Revised March 22, 2015

values of $\sigma_{ln(S)}$ and COV_Q because this results in smaller values for the model uncertainty term $\sigma_{ln(R)}$. These results illustrate how the maximum likelihood analysis of the case history data provides insight on the total uncertainty, but does not itself tightly constrain partitioning of that uncertainty into the components of Q, S, and R.

The solutions based on case histories with FC based on laboratory test data alone (not via correlation to I_c) were not significantly different from those based on all case history data (Figs. 8 and 9). The P_L = 50% curve was about 2% higher and the model uncertainty was slightly smaller.

Solutions were also obtained for those case histories with σ'_v greater than 40 kPa, which excludes cases with representative depths less than about 2 m, where the K_σ and C_N relationships are not as well defined and upper limits on their values have been imposed based on judgment and other considerations. The solutions based on cases with σ'_v greater than 40 kPa, compared to those obtained for all case history data, had 12-13% higher P_L = 50% curves and greater model uncertainties ($\sigma_{ln(R)}$ of 0.30-0.36 versus 0.05-0.24). This combination resulted in P_L = 15% curves shifting downward by about 2% whereas the P_L = 85% curve shifted upward by about 28%.

The sensitivity of the solutions to other aspects of the analyses are described in Boulanger and Idriss (2014), including the effects of alternative approaches to handling potential false negatives and false positives, varying the weighting ratio $w_{nonliquefied}/w_{liquefied}$, and varying the limits on the total uncertainty σ_T at high q_{c1Ncs} values. The effects of these other factors on the solutions were generally smaller than those examined above.

Examination of data for potential biases

Distributions of case history data relative to the triggering curves were examined for potential biases with respect to the primary case history parameters. These distributions are illustrated in the electronic Supplement as plots of the case history data across bins of varying FC, M, and σ'_v. These examinations showed no evident biases with regard to these or other case history parameters.

The case history distributions, as shown in the Supplement, provide a basis for understanding how various components of the analysis framework may or may not affect the triggering correlation. For example, the C_N and K_σ parameters become less certain at confining stresses less than about 30 or 40 kPa for a number of technical reasons, and thus their expressions include imposed maximum values that are reached in this stress range. If those imposed maximum value limits were increased, then the data points in the bin for $\sigma'_v \leq 0.4$ atm will move downward or to the right. The reverse is true if the maximum limits were decreased. The position of the triggering curve is, however, better constrained by the case history data for σ'_v greater than 0.4 atm and thus these data are given more weight in determining the final correlation. The r_d parameter, on the other hand, becomes more uncertain as the depth increases and thus variations in this parameter only has significant effects on the data points for σ'_v greater than about 0.8 atm. The data for the σ'_v bins of 0.8-1.2 atm and >1.2 atm are relatively limited and scattered, such that changes in the r_d relationship had no significant effect on the final triggering correlation. In contrast, variations in the MSF parameter were found to have a more significant effect on the triggering correlation because it affected data across all bins. The revised MSF relationship improved the fit of the data points across the various bins of M compared to the use of an MSF relationship that did not include dependence on soil properties.

Recommended relationships

Selecting the most appropriate values for C_o and $\sigma_{\ln(R)}$ from these maximum likelihood solutions involves subjective evaluation of the most appropriate partitioning of the total uncertainty in the liquefaction case history database. This evaluation must also consider the limitations of the statistical models and case history database, including uncertainties that are not explicitly accounted for. Of the various analysis scenarios considered, the scenarios with $\sigma_{\ln(S)}$ = 0.20, COV_Q = 0.20, and P_{min} = 0.05-0.075 are considered most realistic; e.g., $\sigma_{\ln(S)}$ = 0.10, COV_Q = 0.10 and P_{min} = 0.0 are lower than would be reasonably estimated for these parameters based on available literature as discussed previously. The solutions with larger $\sigma_{\ln(S)}$, COV_Q, and P_{min} terms, however, often gave model uncertainties that are smaller than seem reasonable. This apparent discrepancy arises from limitations in the case history database, the analysis method, and the ability to define parameter uncertainties accurately. Taking these factors into consideration, the results presented herein are considered reasonable bounds of different interpretations, from which values of C_o = 2.60 and $\sigma_{\ln(R)}$ = 0.20 are recommended as reasonable for use in forward calculations.

The liquefaction triggering correlation can then be expressed as,

$$CRR_{M=7.5,\sigma'_v=1atm} = \exp\left(\frac{q_{c1Ncs}}{113} + \left(\frac{q_{c1Ncs}}{1000}\right)^2 - \left(\frac{q_{c1Ncs}}{140}\right)^3 + \left(\frac{q_{c1Ncs}}{137}\right)^4 - 2.60 + \varepsilon_{\ln(R)}\right) \quad (33)$$

where $\varepsilon_{\ln(R)}$ is normally distributed with a mean of 0.0 and a standard deviation of $\sigma_{\ln(R)}$ = 0.20. This expression can also be written as,

$$CRR_{M=7.5,\sigma'_v=1atm} = \exp\left(\frac{q_{c1Ncs}}{113} + \left(\frac{q_{c1Ncs}}{1000}\right)^2 - \left(\frac{q_{c1Ncs}}{140}\right)^3 + \left(\frac{q_{c1Ncs}}{137}\right)^4 - 2.60 + \sigma_{\ln(R)} \cdot \Phi^{-1}\left(P_L\right)\right) \quad (34)$$

where Φ^{-1} is the inverse of the standard cumulative normal distribution, and P_L is the probability of liquefaction. Alternatively, the conditional probability of liquefaction for known values of $CSR_{M=7.5,\sigma'=1atm}$ and q_{c1Ncs} can be computed as,

$$P_L\left(q_{c1Ncs}, CSR_{M=7.5,\sigma'_v=1atm}\right) = \Phi\left[-\frac{\frac{q_{c1Ncs}}{113} + \left(\frac{q_{c1Ncs}}{1000}\right)^2 - \left(\frac{q_{c1Ncs}}{140}\right)^3 + \left(\frac{q_{c1Ncs}}{137}\right)^4 - 2.60 - \ln\left(CSR_{M=7.5,\sigma'_v=1atm}\right)}{\sigma_{\ln(R)}}\right] \quad (35)$$

The recommended triggering curves for P_L equal to 15%, 50%, and 85% with model uncertainty

Submitted September 2014
Revised March 22, 2015

alone [i.e., conditional on known values of $CSR_{M=7.5,\sigma'=1atm}$ and q_{c1Ncs}] are plotted together with the clean sand (FC ≤ 5%) case history data in Fig. 11a and the full case history database in Fig. 11b. For deterministic analyses, it is recommended that the P_L = 15% curve be used (i.e., approximately one standard deviation below the mean; Equation 34 with $\varepsilon_{ln(R)}$ = -0.20).

The probabilistic triggering relationship expressed in Equations 33-35 is conditional on known values for $CSR_{M=7.5,\sigma'=1atm}$ and q_{c1Ncs} values. Therefore, to assess the probability of liquefaction in a hazard evaluation, the conditional probability of liquefaction provided by these equations needs to be combined with the probabilities of the $CSR_{M=7.5,\sigma'=1atm}$ and q_{c1Ncs} values; i.e., the parameter uncertainties. The uncertainties in estimating the latter parameters are often greater than the uncertainty in the triggering model, such that the formal treatment of uncertainties in the seismic hazard analysis and a detailed site characterization effort are generally more important to a probabilistic liquefaction analysis than the uncertainty in the liquefaction triggering model.

For example, a probabilistic liquefaction hazard analysis can be structured to branch through a range of seismic hazards (accounting for the majority of uncertainty in $CSR_{M=7.5,\sigma'=1atm}$ values) and a range of site characterizations (accounting for the majority of the uncertainty in the q_{c1Ncs} values) before it gets to the liquefaction triggering analysis. In that scenario, it may be reasonable to only include model uncertainty in the liquefaction triggering analysis because the parameter uncertainties were already accounted for in the previous branches of the analysis.

Summary

A probabilistic CPT-based liquefaction triggering correlation was developed using an updated case history database and a maximum likelihood approach. The liquefaction analysis framework followed that by Idriss and Boulanger (2008) and incorporated changes to the MSF relationship and the procedures for estimating FC from the I_c index when site specific sampling and lab testing data are not available. The revised correlation was shown to exhibit no apparent trends or biases relative to the case history data with respect to FC, M, or σ'_v.

For analyses in the absence of site-specific lab testing data, it is suggested that liquefaction analyses be repeated using a range of C_{FC} values (e.g., ±0.15 or ±0.29) to evaluate the sensitivity to FC estimates and a range of I_c cut-off values for identifying clay-like soils (e.g., 2.4 versus 2.6) to evaluate sensitivity to soil classification estimates. The results can be used to evaluate the potential benefits of site-specific sampling and testing for a given project, while recognizing that some amount of sampling and testing should be required for high risk/high consequence projects.

Measurement and estimation uncertainties in CSR and q_{c1Ncs}, the potential effects of false positives and false negatives in the case history database, and the effects of the choice-based sampling bias in the case history database were accounted for. The results of sensitivity analyses showed that the position of the most likely triggering curve and the magnitude of the total error term were well constrained by the data. The most likely value for the standard deviation of the error term in the triggering correlation was, however, found to be dependent on the uncertainties assigned to CSR and q_{c1Ncs} and the potential presence of false negatives and false positives in the case history database. Despite this and other limitations, the results of the sensitivity study appear to provide reasonable bounds on the effects of different interpretations. The probabilistic relationship for liquefaction triggering proposed herein is considered a reasonable approximation in view of these various findings.

Probabilistic liquefaction hazard analyses should consider the uncertainties in the seismic hazard, the site characterization, and the liquefaction triggering model. The uncertainty in the liquefaction triggering model is smaller than the uncertainty in the seismic hazard, and will often be smaller than the uncertainty in the site characterization. For this reason, the seismic hazard analysis and the site characterization efforts are often the more important components of any probabilistic assessment of liquefaction hazards.

ACKNOWLEDGMENTS

The authors are grateful for information and insights from numerous colleagues. Information on case histories was provided by Drs. Michael Bennett, Thomas Holzer, and Rob Kayen. Professor Russell Green and his coauthors provided advance copies of their work examining CPT data from Christchurch. Comments were provided by Professors Jonathan Bray, Misko Cubrinovski, Jason DeJong, Russell Green, James Mitchell, and Jonathan Stewart, Drs. Mike Beaty, Dave Gillette, Thomas Holzer, Lelio Mejia, and Peter Robertson, and Mr. Adam Price. The authors are, however, solely responsible for the data, interpretations, and recommendations presented herein.

Portions of this work were supported by the California Department of Water Resources (DWR) and National Science Foundation (grants CMMI-1138203 and CMMI-1300518). Any opinions, findings, or recommendations expressed in this material are those of the authors and should not be interpreted as representing the official policies, either expressed or implied, of either organization.

REFERENCES

Abrahamson, N., Atkinson, G., Boore, D., Bozorgnia, Y., Campbell, K., Chiou, B., Idriss, I. M., Silva, W., and Youngs, R. (2008). "Comparisons of the NGA ground-motion relations." Earthquake Spectra, 24(1), 45-66.

Ancheta, T. D., Darragh, R. B., Stewart, J. P., Seyhan, E., Silva, W. J., Chiou, B. S. J., Wooddell, K. E., Graves, R. W., Kottke, A. R., Boore, D. M., Kishida, T., and Donahue, J. L. (2014). "NGA-West 2 database." Earthquake Spectra, EERI, dx.doi.org/10.1193/070913EQS197M.

Baecher, G. B., and Christian, J. T. (2003). Reliability and Statistics in Geotechnical Engineering. John Wiley and Sons, Ltd., 619 pp.

Boulanger, R. W. (2003). High overburden stress effects in liquefaction analyses, *J. Geotechnical and Geoenvironmental Eng.,* ASCE **129**(12), 1071–082.

Boulanger, R. W., and Idriss, I. M. (2012). "Probabilistic SPT-based liquefaction triggering procedure." *J. Geotechnical and Geoenvironmental Eng.*, ASCE, 138(10), 1185-1195.

Boulanger, R. W., and Idriss, I. M. (2014). "CPT and SPT based liquefaction triggering procedures." Report No. UCD/CGM-14/01, University of California, Davis, CA, 134 pp.

Boulanger, R. W., and Idriss, I. M. (2015). "Magnitude scaling factors in liquefaction triggering procedures." Soil Dynamics and Earthquake Engineering, 10.1016/j.soildyn.2015.01.004.

Cetin, K. O., Der Kiureghian, A., Seed, R. B. (2002). "Probabilistic models for the initiation of seismic soil liquefaction." Structural Safety, 24: 67-82.

Cetin, K. O., Seed, R., Der Kiureghian, A., Tokimatsu, K., Harder, L., Kayen, R., Moss, R. E. S. (2004). Standard penetration test-based probabilistic and deterministic assessment of seismic soil liquefaction potential, *J. Geotechnical and Geoenvir. Eng.*, ASCE **130**(12), 1314–340.

Christian, J. T., and Swiger, W. F. (1975). "Statistics of liquefaction and SPT results." Journal of Geotechnical Engineering Div., ASCE, 101(GT11), 1135-1150.

Cox, B. R., et al. (2013). "Liquefaction at strong motion stations and in Urayasu City during the 2011 Tohoku-Oki earthquake." Earthquake Spectra, EERI, 29(S1), S55-S80.

Engdahl, E. R., and Villasenor, A. (2002). "Global seismicity: 1900-1999." Intl Handbook of Earthquake and Engineering Seismology, Committee on Education, Vol. 81A, 665-690.

Green, R. A., Cubrinovski, M., Cox, B., Wood, C., Wotherspoon, L., Bradley, B., and Mauer, B. (2014). "Select liquefaction case histories from the 2010-2011 Canterbury earthquake sequence." Earthquake Spectra, EERI, http://dx.doi.org/10.1193/030713EQS066M.

Idriss, I. M. (1999). An update to the Seed-Idriss simplified procedure for evaluating liquefaction potential, *Workshop on New Approaches to Liquefaction*, Publication No. FHWA-RD-99-165.

Idriss, I. M., and Boulanger, R. W. (2004). Semi-empirical procedures for evaluating liquefaction potential during earthquakes, *11th Intl Conf Soil Dynamics and Earthquake Engrg, and 3rd Intl Conf Earthquake Geotechnical Engrg*, D. Doolin et al., eds., Stallion Press, Vol. 1, pp. 32–56.

Idriss, I. M., and Boulanger, R. W. (2008). *Soil liquefaction during earthquakes*. Monograph MNO-12, Earthquake Engineering Research Institute, Oakland, CA, 261 pp.

Idriss, I. M., and Boulanger, R. W. (2010). "SPT-based liquefaction triggering procedures." Report UCD/CGM-10/02, Center for Geotechnical Modeling, Univ. of California, Davis, CA, 259 pp.

Juang, C. H., Jiang, T., and Andrus, R. D. (2002). "Assessing probability-based methods for liquefaction potential evaluation." *J. Geotechnical and Geoenv. Eng.*, ASCE, 128(7), 580-589.

Kulhawy, F. H. and Trautmann, C. H. (1996). "Estimation of in-situ test uncertainty." Uncertainty in the Geologic Environment, Madison, WI, ASCE: 269–286.

Liao, S. S. C., and Lum, K. Y. (1998). "Statistical analysis and application of the magnitude scaling factor in liquefaction analysis." Geotech. Earthquake Eng. and Soil Dyn. III, ASCE, 1:410–21.

Liao, S. S. C., Veneziano, D., and Whitman, R. V. (1988). "Regression models for evaluating liquefaction probability." J. Geotech. Eng. Div., ASCE, 114(4), 389–411.

Manski, C. F., and Lerman, S. R. (1977). "The estimation of choice probabilities from choice-based samples." Econometrica, 45(8): 1977-1998.

Mitchell, J. K., and Tseng, D. J. (1990). "Assessment of liquefaction potential by cone penetration resistance", Proc., H. Bolton Seed Memorial Symposium, BiTech Publishers, Vol. 2, 335-350.

Montgomery, J., Boulanger, R. W., and Harder, L. F., Jr. (2014). "Examination of the K□ overburden correction factor on liquefaction resistance." *J. Geotechnical and Geoenvironmental Eng.*, ASCE, dx.doi.org/10.1061/(ASCE)GT.1943-5606.0001172.

Moss, R. E. S., Seed, R. B., Kayen, R. E., Stewart, J. P., Youd, T. L., and Tokimatsu, K. (2003). "Field case histories for CPT-based in situ liquefaction potential evaluation." Geoengineering Research Rep. UCB/GE-2003/04, University of California, Berkeley.

Moss, R. E. S., Seed, R. B., Kayen, R. E., Stewart, J. P., Der Kiureghian, A., and Cetin, K. O. (2006). CPT-based probabilistic and deterministic assessment of in situ seismic soil liquefaction potential, *J. Geotechnical and Geoenvironmental Eng.*, ASCE **132**(8), 1032–051.

Nguyen, T., Shao, L., Gingery, J., Robertson, P. (2014). "Proposed modification to CPT-based liquefaction method for post-vibratory ground improvement." Geo-Congress 2014, 1120-1132.

PEER (2000a). "Documenting incidents of ground failure resulting from the Aug. 17, 1999, Kocaeli, Turkey Earthquake." peer.berkeley.edu/publications/turkey/adapazari/ (9/2013).

PEER (2000b). "Documentation of soil conditions at liquefaction sites from 1999 Chi-Chi, Taiwan Earthquake." peer.berkeley.edu/lifelines/research_projects/3A02/ (last accessed 9/2013).

Phoon, K. K. and Kulhawy, F. H. (1999). "Characterization of geotechnical variability." Canadian Geotechnical Journal 36(4): 612–624.

Robertson, P. K., and Wride, C. E. (1998). "Evaluating cyclic liquefaction potential using the cone penetration test." Canadian Geotechnical J. 35(3), 442–59.

Robinson, K., Cubrinovski, M., and Bradley, B.A. (2013). "Comparison of actual and predicted measurements of liquefaction-induced lateral displacements from the 2010 Darfield and 2011 Christchurch Earthquakes." Proc. 2013 Conference of the New Zealand Society for Earthquake Engineering (NZSEE 2013), Wellington, New Zealand, 26-28 April.

Sancio, R. B. (2003). Ground failure and building performance in Adapazari, Turkey. Ph.D. thesis, University of California, Berkeley, 790 pp.

Suzuki, Y., Tokimatsu, K., Taya, Y., and Kubota, Y. (1995). "Correlation between CPT data and dynamic properties of in situ frozen samples." Proc., 3rd International Conference on Recent Advances in Geotechnical Earthquake Engineering and Soil Dynamics, Vol. I, St. Louis, MO.

Suzuki Y., Sanematsu, T., and Tokimatsu, K. (1998). "Correlation between SPT and seismic CPT." Proc., Conference on Geotechnical Site Characterization, Balkema, Rotterdam, pp. 1375–380.

Tokimatsu, K., Tamura, S., Suzuki, H., and Katsumata, K. (2012). "Building damage associated with geotechnical problems in the 2011 Tohoku Pacific Earthquake." Soils and Foundations, Japanese Geotechnical Society, 52(5): 956-974.

Toprak, S., Holzer, T. L., Bennett, M. J., Tinsley, J. C. (1999). "CPT- and SPT-based probabilistic assessment of liquefaction potential." Report MCEER-99-0019, MCEER, NY.

Van Ballegooy, S., Malan, P., Lacrosse, V., Jacka, M. W., Cubrinovski, M., Bray, J. D., O'Rourke, T. D., Crawford, S. A., and Cowan, H. (2014). "Assessment of liquefaction-induced land damage for residential Christchurch." Earthquake Spectra, EERI, in-press.

Worden, C. B., Wald, D. J., Allen, T. I., Lin, K., and Cua, G. (2010). "Integration of macroseismic and strong-motion earthquake data in ShakeMap for real-time and historic earthquake analysis." USGS web site, http://earthquake.usgs.gov/earthquakes/shakemap/.

Youd, T. L, and Noble, S. K. (1997). "Liquefaction criteria based on statistical and probabilistic analyses." Report NCEER-97-022, NCEER, 201–205.

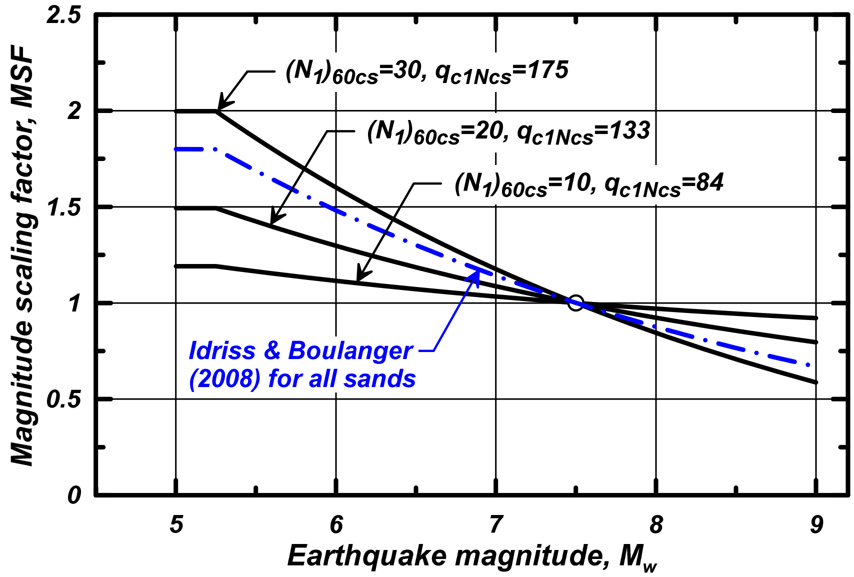

Fig. 1. Variation in the MSF relationship with q_{c1Ncs} and with $(N_1)_{60cs}$ for cohesionless soils

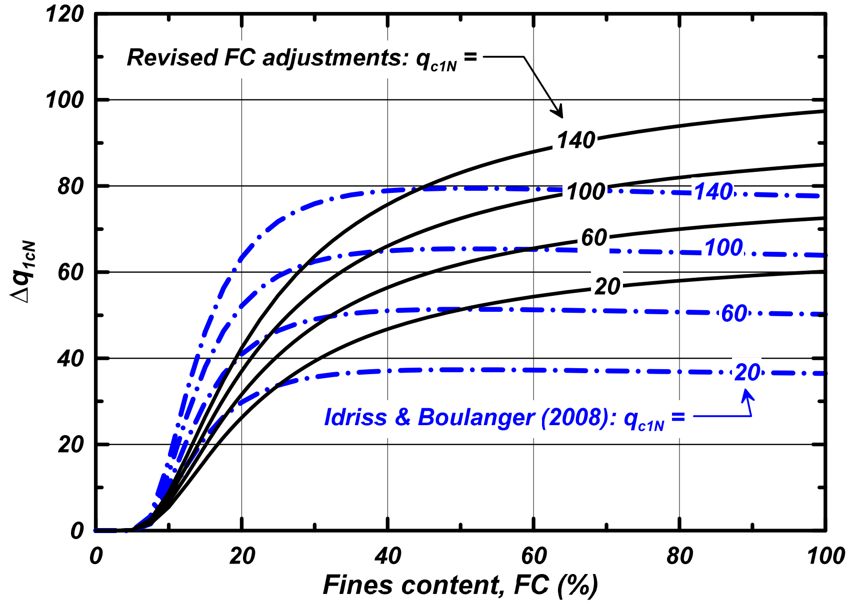

Fig. 2. Equivalent clean sand adjustments for CPT-based liquefaction triggering procedures

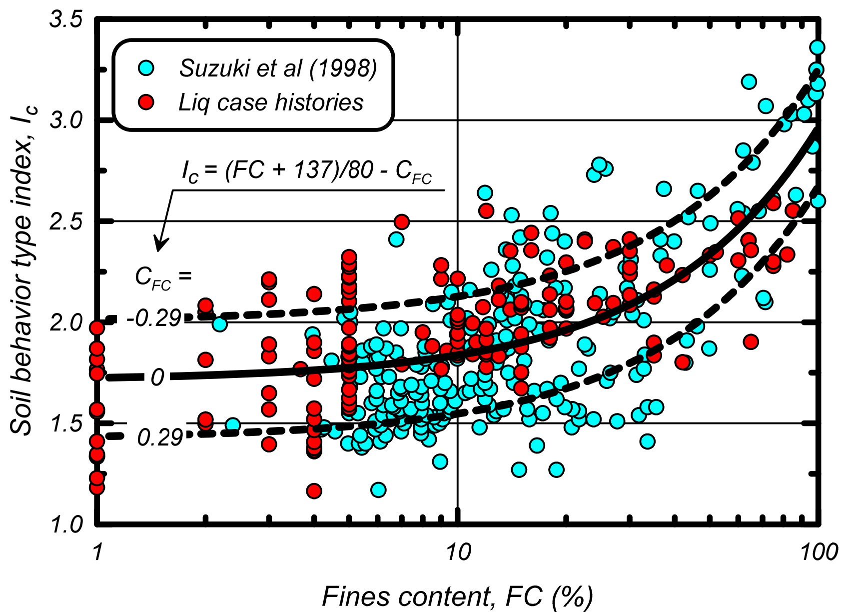

Fig. 3. Recommended correlation between I_c and FC with plus or minus one standard deviation against the dataset by Suzuki et al. (1998) and the liquefaction database

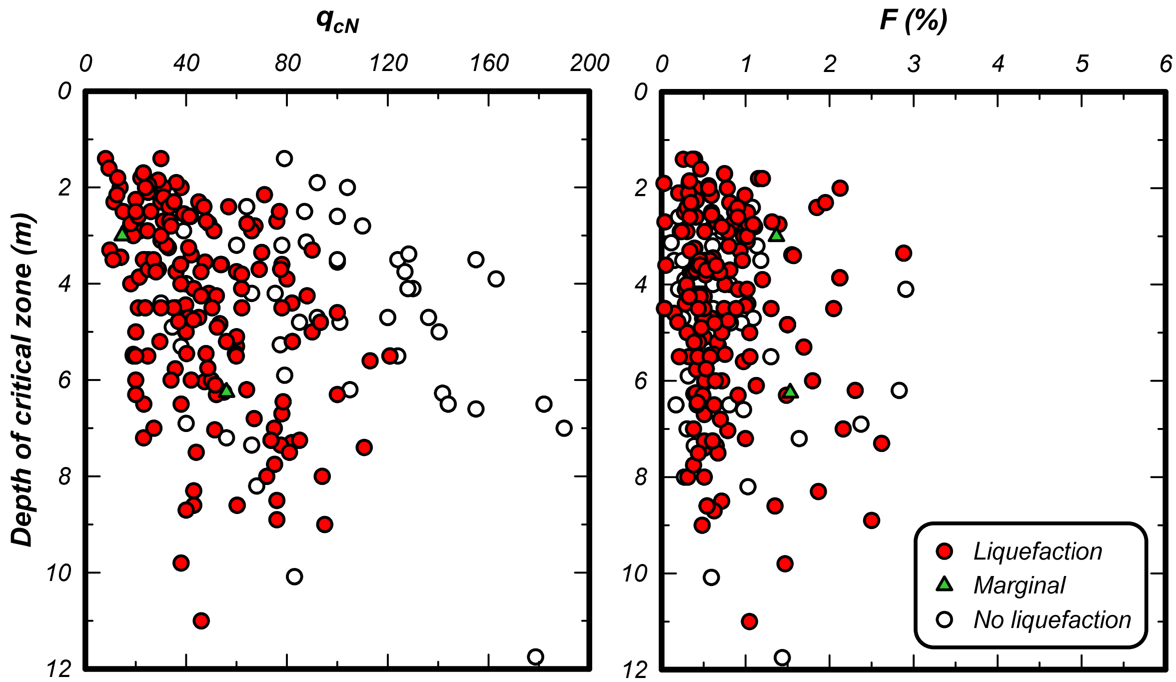

Fig. 4. Distributions of q_{cN} and F versus the representative depth of the critical zone

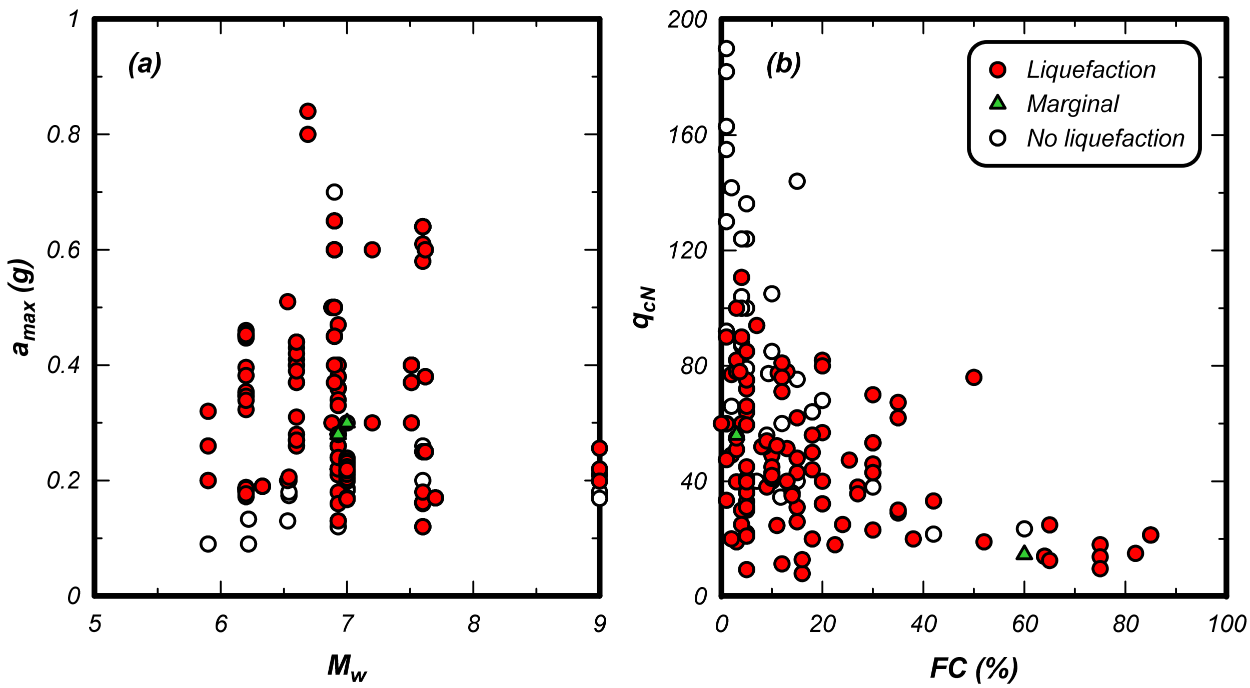

Fig. 5. Distributions of: (a) a_{max} versus M and (b) q_{cN} versus FC for cases with FC determined by laboratory testing

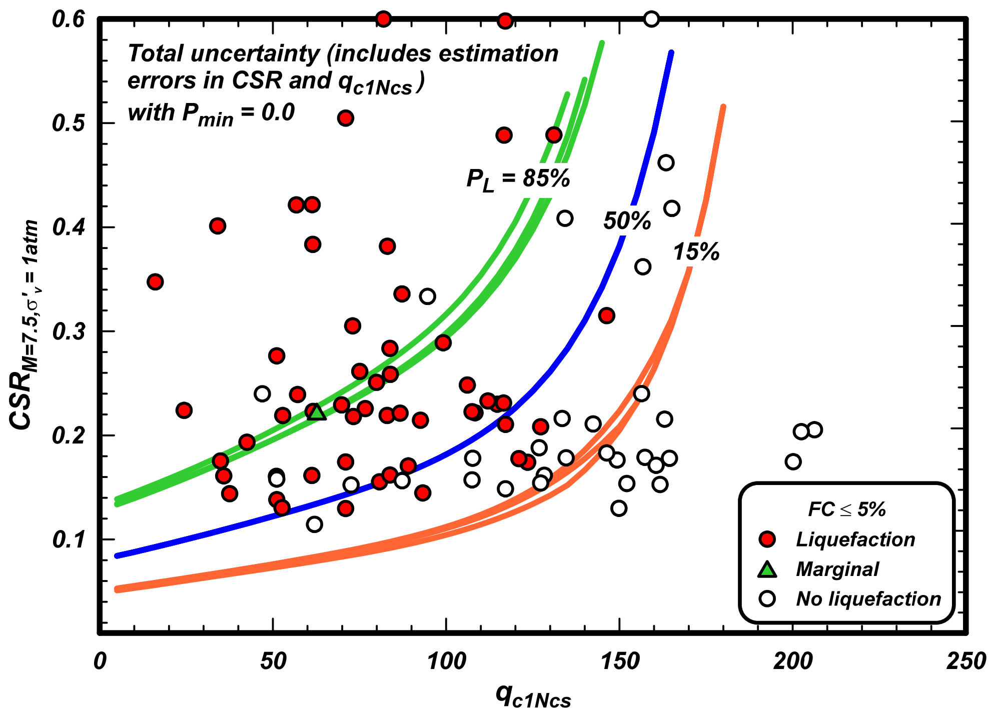

Fig. 6. $CRR_{M=7.5,\sigma'v=1atm}$ versus q_{c1Ncs} for P_L = 15, 50, and 85% in clean sands with inclusion of estimation errors in $CSR_{M=7.5,\sigma'v=1atm}$ and q_{c1Ncs} and using P_{min} = 0.0

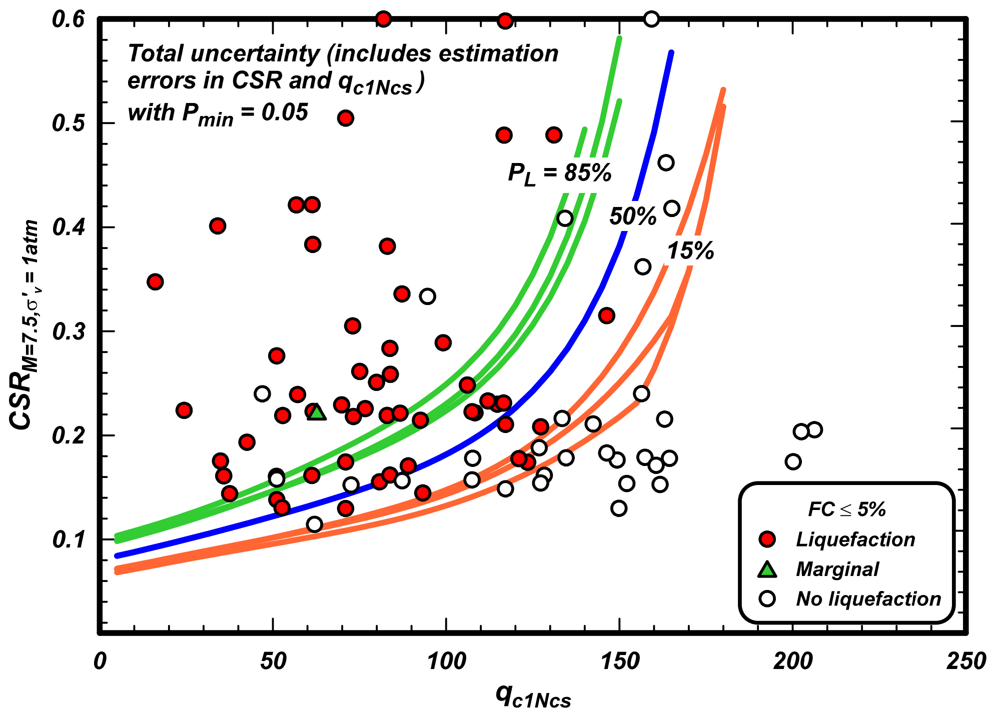

Fig. 7. $CRR_{M=7.5,\sigma'v=1atm}$ versus q_{c1Ncs} for P_L = 15, 50, and 85% in clean sands with inclusion of estimation errors in $CSR_{M=7.5,\sigma'v=1atm}$ and q_{c1Ncs} and using P_{min} = 0.05

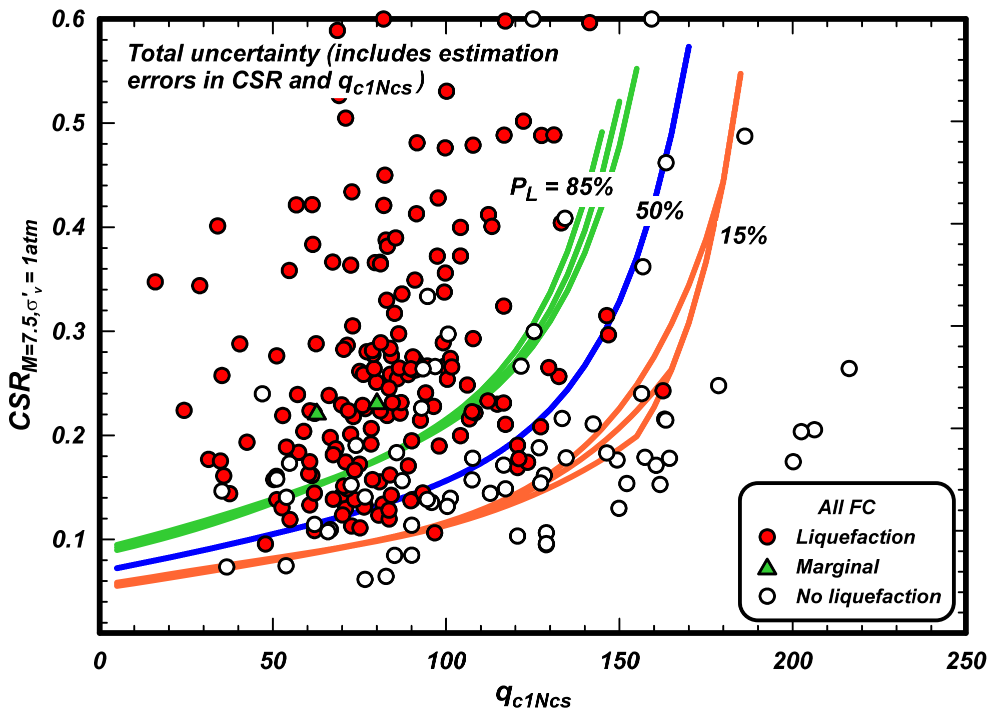

Fig. 8. $CRR_{M=7.5,\sigma'v=1atm}$ versus q_{c1Ncs} for P_L = 15, 50, and 85% for all sands with inclusion of estimation errors in $CSR_{M=7.5,\sigma'v=1atm}$ and q_{c1Ncs} with P_{min} = 0.075

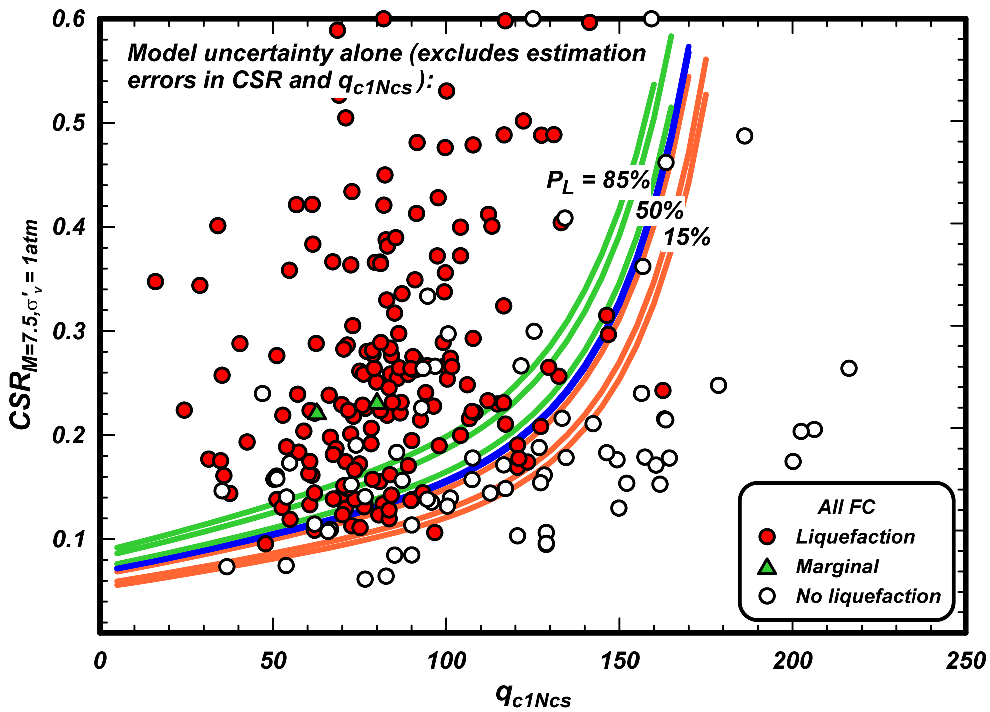

Fig. 9. $CRR_{M=7.5,\sigma'v=1atm}$ versus q_{c1Ncs} for P_L = 15, 50, and 85% for all sands with model uncertainty alone (excluding estimation errors in $CSR_{M=7.5,\sigma'v=1atm}$ and q_{c1Ncs}) with P_{min} = 0.075

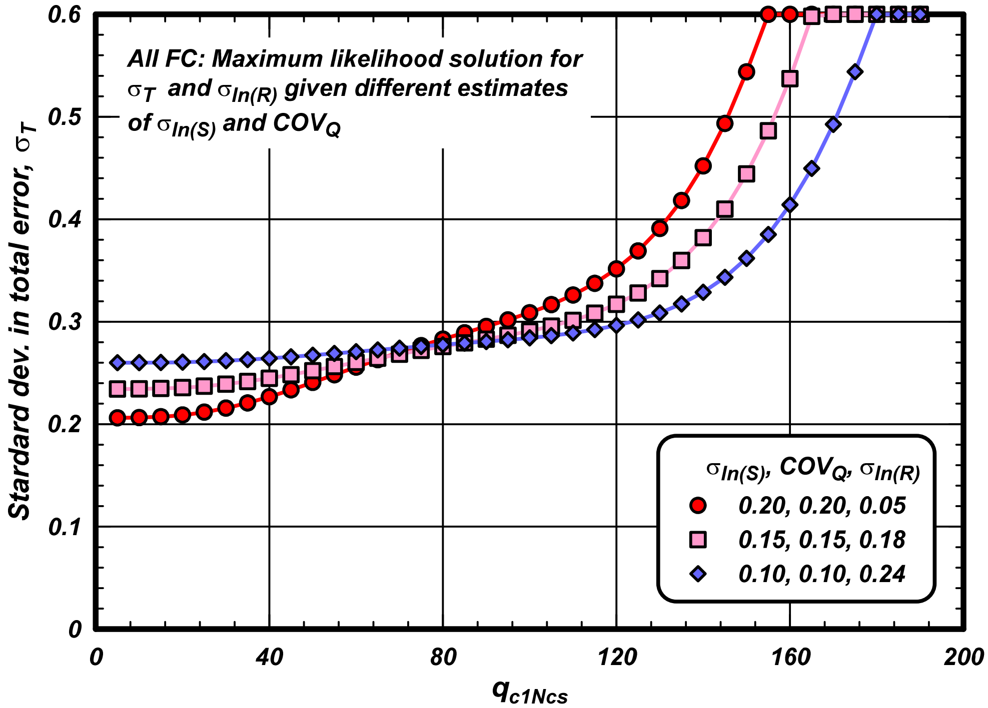

Fig. 10. Standard deviation in the total error term (σ_T) and CRR relationship ($\sigma_{\ln(R)}$) for different estimates of $\sigma_{\ln(S)}$ and COV_Q in any FC sand with $P_{min} = 0.075$

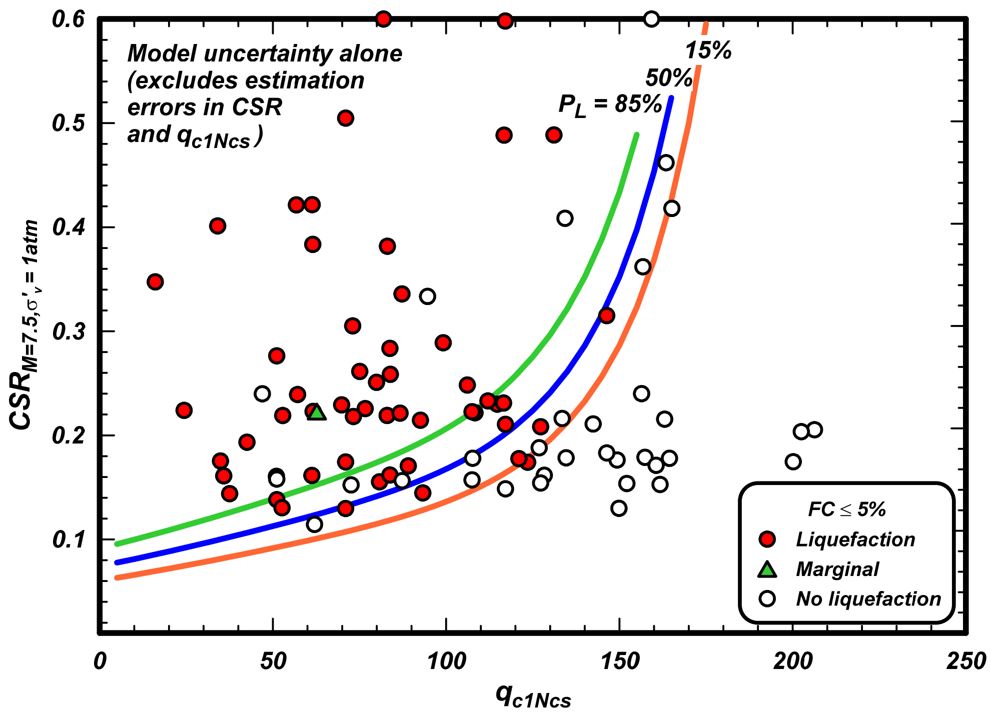

(a)

Fig. 11. Curves of $CRR_{M=7.5,\sigma'v=1atm}$ versus q_{c1Ncs} for probabilities of liquefaction of 15%, 50%, and 85%: (a) clean sands, (b) all sands

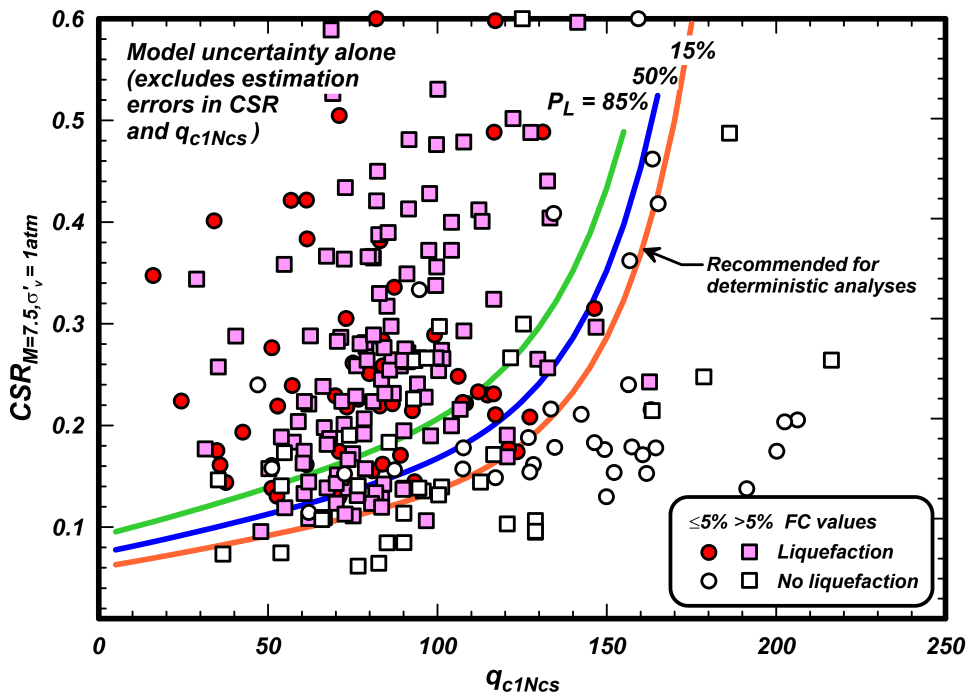

(b)

Fig. 11. Curves of $CRR_{M=7.5,\sigma'v=1atm}$ versus q_{c1Ncs} for probabilities of liquefaction of 15%, 50%, and 85%: (a) clean sands, (b) all sands